SEMARAK ILMU PUBLISHING

Journal of Advanced Research in Fluid Mechanics and Thermal Sciences

Journal homepage:
https://semarakilmu.com.my/journals/index.php/fluid_mechanics_thermal_sciences/index
ISSN: 2289-7879

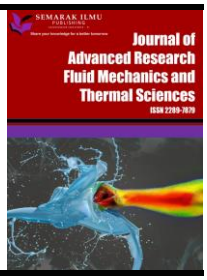


# The Foundation and Validation of Sigmoid-Typed Functions for Fouling Formation Modelling of Crude Oil Flows

Gunawan Nugroho[1,*], Novandion R. Kurniawan[1], Totok R. Biyanto[1], Purwadi A. Darwito[1], Titik Budiati[2]

[1] Department of Engineering Physics, Institut Teknologi Sepuluh Nopember, Kampus ITS Sukolilo, Surabaya, 60111, Indonesia
[2] Department of Food Engineering, Politeknik Negeri Jember, Jl. Mastrip, Jember, 68121, Indonesia

**ARTICLE INFO**

***Article history:***
Received 17 June 2023
Received in revised form 10 September 2023
Accepted 20 September 2023
Available online 9 October 2023

***Keywords:***
Heat Exchanger; fouling formation; sigmoid function; crude oil flows

**ABSTRACT**

The phenomenological model of fouling formation is investigated in this research which, the parametrization method based on the species and energy equation is implemented. It is shown that the previous empirical sigmoid-typed correlation can also be generated from the species equation as a special solution. Meanwhile, the fouling heat resistance is obtained from the phenomenological energy equation. Correlating these two solutions, it is shown that the proposed model generates key parameters of fouling formation characteristics of crude preheat train within all operational conditions. Thus, it generalizes the previous models as it covers wider operational range.

## 1. Introduction

Heat exchanger has a crucial role as heat transfer equipment in many industrial processes. Various designs have the flexibility to adapt into many industrial processes based on thermodynamics properties, temperature, pressure, fluids, stream phase, density, chemical composition and viscosity [1]. As a preheat train in crude oil refining process, it is fed by heating fluid in the network coming from downstream products, which the recovered heat can be considered as energy saving [2]. However, fouling is the main problem in this specific application because details of physical and chemical mechanisms in fouling formation are not clear and depend on several conditions. Operational and financial from refinery unit are affected by formation of fouling as it causes losses in thermal efficiency, constriction of pipe cross-section, increasing pressure drop as well as increasing maintenance cost, which are major impacts from fouling formation [3]. Fouling formation occurs in various forms, such as chemical reaction, corrosion, crystallization, particulate, biological, solidification and combine fouling. It is pointed that variation of heat transfer surface and bulk fluid

* *Corresponding author.*
*E-mail address: gunawan@ep.its.ac.id*

https://doi.org/10.37934/arfmts.110.1.104120

temperature are the fundamental variables which significantly lead to crystallization, chemical reaction and biological fouling [4].

Some scrutinized studies have predicted the behavior of the fouling formation based on semi-empirical model [5–10]. All of them are based on two basic mechanisms, i.e., deposition and removal terms, though it has different determination on physical mechanisms that drive the processes. Operational variables such as temperature, flow velocity, concentration and material surfaces play significant role on retardation of fouling and particulate deposition [4]. Deposit formation was observed increasing with temperature at fixed flow velocity [11], but the surface temperature of deposit usually decreases as fouling layer grows even though the wall temperature increase [12]. On the other side, removal term is highly susceptible to flow geometry and this led the need to convert a scaling factor by comparing experimental data toward different geometries [13]. The Other factors are due to filterable solids present in the opportunity crudes, velocity driven deposit, crude incompatibility, thermal degradation and solubility crude blending [14].

The practical fouling model needs to cover all aspects mechanism involved during fouling development process. Recent consideration to describe deposition term may come up with introducing temperature dependent of crude oil properties to involve physical processes factor [13]. The challenges also come from the shifting balance between thermal and hydraulic impacts of fouling caused by ageing that may cause error in estimating foulant layer due to increase of thermal conductivity [15]. Recent empirical study shows that fouling resistance phenomena also can be described through Sigmoidal-Boltzmann model as it is based on recent data [16]. The practical success of sigmoid-typed empirical model motivates the study of its phenomenology based on the governing equations. Further analysis will be conducted in this paper.

## 2. Methodology

### *2.1 Reviews on Empirical Crude Oil Fouling Models*

Generally, recent semi-empirical model is based on net fouling rate that is defined as difference between the deposition and the removal rate,

$$\frac{dR_f}{dt} = Deposition - Removal \tag{1}$$

The first semi-empirical model was proposed by Ebert-Panchal [5] which is triggered by two mechanisms. The first term is related to chemical reactions (deposition) and the second term related to shear stress which remove the fouling (removal). The activation energy obtained from the gradient of Arrhenius plot between fouling resistance rate and $1/T_f$, each are in log-scale.

$$\frac{dR_f}{dt} = nPr^{-0.33}\ \exp\left(\frac{-E}{RT_f}\right) - \gamma\tau_w \tag{2}$$

The shear stress in tube is given by,

$$\tau_w = f\frac{\rho u^2}{2} \tag{3}$$

and for Fanning frictional factor, there are various equations to estimate the value. In this case we are using the equation proposed by Saunders [17].

$$f = 0.0035 + \frac{0.264}{Re^{0.42}} \tag{4}$$

Fouling assumed occurs in temperature film region, weighted from between wall temperature and bulk temperature.

$$T_f = T_b + 0.55(T_w - T_b) \tag{5}$$

Ebert-Panchal model has been developed by Polley *et al.,* [6], that criticize an exponent power of Reynolds Number in deposition. Polley *et al.,* expected that value of exponential power was 0.88 rather than 0.66 in the case of turbulent flow in circular pipe. Another modification from Ebert-Panchal model is the shear stress is proportional only to $Re^{0.88}$ and temperature used in Arrhenius exponential is depending on wall temperature instead of film temperature, which resulted in,

$$\frac{dR_f}{dt} = nPr^{-0.33} \exp\left(\frac{-E}{RT_w}\right) - \gamma Re^{0.8} \tag{6}$$

The model of Polley *et al.,* has been improved by Nasr-Givi [7] by simplification of deposition term that it depends only on Reynolds number with adjustable exponential power and Arrhenius constants. Meanwhile, film temperature was implemented in this model rather than using wall temperature. For removal term, $Re^{0.4}$ is used which is replacing the $Re^{0.8}$ term. Thus, the model becomes,

$$\frac{dR_f}{dt} = nRe^{\beta} \exp\left(\frac{-E}{RT_f}\right) - \gamma Re^{0.4} \tag{7}$$

Following that relation, Shetty *et al.,* [8] proposed the use of effective temperature to find the proper weight between surface and bulk temperature. In the study of Deshannavar-Ramasamy [9], it is found that both temperature and flow rate affect the activation energy as determined by their formula. Continuing the work from Saleh-Sheikholeslami [17,18], Farahbod-Karazhian proposed a new fouling model which consider the operational pressure and velocity in deposition term. However, Nasr-Givi model shows the simplest form among the existing models and this will be involved in our proposed a new crude oil fouling model.

Recent study shows that fouling resistance tend to follow sigmoidal curve rather than linear curve inherited by any existing semi-empirical model [16]. Various types of sigmoidal function already exist. One of them is Sigmoidal-Boltzmann function which the time-function expression of Sigmoidal-Boltzmann depend on the four-parameters as follows,

$$y = A_2 + \frac{A_1 - A_2}{1 + e^{\left(\frac{t - t_c}{b_s}\right)}} \tag{8}$$

where $A_1$, $A_2$ are the initial and final value respectively, $t_c$ is time characteristic of curve (midpoint of curve) and $b_s$ is time constant represents the gradient of slope near $t_c$.

Fouling resistance depends on heat transfer process and fouling mechanism accompanied by itself. The observation of fouling resistance over time shows different characteristics. The strength of deposition and removal terms play a role to determine these characteristics. The weaker the

deposition term, fouling resistance curve will tend to be asymptotic, and stronger deposition lead to shows the linear or fouling-rate curve [19]. The importance of Sigmoidal-Boltzmann function is, it can cover three empirical trends of fouling resistance, i.e., asymptotic, linear and falling rate by choosing appropriate parameters. Lower $t_c$ will eliminate initiation period and the curve tends to be asymptotic. Another case where $b_s$ is large such that the curve tends to be linear.

Therefore, based on these information of fouling curve and physical parameters (Figure 1), empirical model cannot be neglected, such that a new model based on empirical model and phenomenological model is proposed to predict crude oil fouling.

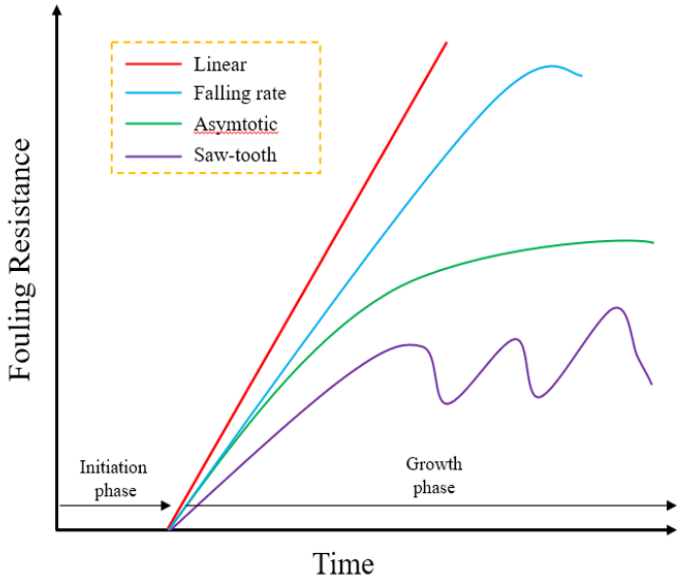


**Fig. 1.** Fouling resistance curve

*2.2 The Phenomenological Foundation*

In this work, the fouling accumulation due to chemical reaction is described by the continuity equation as,

$$m_t = \dot{m}_{in} - \dot{m}_{out} + \dot{m}_{gen} \tag{10}$$

with, $\dot{m}_t$ and $\dot{m}_{gen}$ are mass accumulation inside the control volume and mass generation which will become as a source term from chemical reaction. The above equation can be expanded into first order PDE and leads to continuity equation and then, species equation of reaction-diffusion. Thus, based on Fisher-Kolmogorov-Petrowskii-Piscounov (FKPP) equation [20] which introduce $R(Y_f) = h\rho u Y_f + k\rho Y_f^2$ as a non-linear source term, the species equation is,

$$\rho \frac{\partial Y_f}{\partial t} = \rho D \frac{\partial^2 Y_f}{\partial x^2} + R(Y_f) \tag{11}$$

where, $h$ is flow constant, $k$ is the reaction constants and $D$ is the species diffusivity. The first term in $R(Y_f)$ is related to convective term and the second term is related to fouling mass generation due to chemical reaction. Eq. (11) can be expressed in lumped mass fraction as follows,

$$\left(\rho Y_f\right)_t = h\rho u Y_f + k\rho Y_f^2 - \rho C \tag{12}$$

which the process is assumed as constant diffusion and is related to the fouling removal, $D\frac{\partial^2 u}{\partial x^2} = -C$. Thus, species conservation equation is rewritten as,

$$Y_{ft} = huY_f + kY_f^2 - C \tag{13}$$

or in another form, it is rewritten as,

$$Y_{ft} = \left(kY_f + a\right)\left(Y_f - b\right) \tag{14}$$

where $a - kb = hu$ and $ab = C$. Integration of the above equations gives,

$$\left[\frac{1}{\left(kY_f + a\right)} - \frac{\rho}{k\left(Y_f - b\right)}\right]\partial Y_f = \partial t \tag{15}$$

here, $\frac{1}{k}a + b = -1$, then combine with $a - b = hu$ resulting $b = -\frac{(k+hu)}{k+1}$ and $a = k\frac{(k+hu)}{k+1} - k$ Then, $C = k\left[\frac{(k+hu)}{k+1} - \frac{(k+hu)^2}{(k+1)^2}\right]$. The solution from this species equation is,

$$\ln\frac{\left(Y_f + \frac{a}{k}\right)^{\frac{1}{k}}}{\left(Y_f - b\right)} = t \quad or \quad \left(Y_f + \frac{a}{k}\right) = e^{kt}\left(Y_f - b\right)^k \tag{16}$$

Since $k = 1$ is generally used in kinetics of fouling formation, the solution of mass fraction is given by,

$$Y_f = \frac{be^t + a}{e^t - 1} \tag{17}$$

Then, fouling mass fraction is expressed as,

$$m_f = m_{tot}Y_f = m_{tot}\left(\frac{be^t + a}{e^t - 1}\right) \tag{18}$$

The fouling mass here will contribute to heat conduction resistance, which the relation to the fouling mass fraction is derived as,

$$L_f = \frac{m_f}{\rho A} = \frac{m_{tot}}{\rho A}\left(\frac{be^t + a}{e^t - 1}\right) \tag{19}$$

yielding formulation of thermal resistance as follows.

$$R_f = \frac{L_f}{K_f A} = \frac{1}{K_f A}\frac{m_{tot}}{\rho A}\left(\frac{be^t + a}{e^t - 1}\right) \tag{20}$$

with $K_f$ is fouling thermal conductivity and $A$ is heat transfer area.

The step now is to consider the energy equation. Since at the fouling growth state, the reaction time has its own dynamics and much faster than heat transfer and hydrodynamic times. Thus, energy equation can be observed in steady state balance as follows [21],

$$u\frac{\partial T}{\partial x} = \frac{\alpha}{r}\frac{\partial}{\partial r}\left(r\frac{\partial T}{\partial r}\right) - \overline{u'\frac{\partial T'}{\partial x}} + \Phi_{dissp} \tag{21}$$

with, $\alpha = \frac{\lambda}{\rho c_p}$, which $\alpha$ is heat diffusion coefficient, $\rho$ is fluid density, $\lambda$ is fluid thermal conductivity and $c_p$ is fluid specific heat. The two last terms are contribution of turbulent heat convection and dissipation of mechanical energy in fluid due to shear stress. Substitute the velocity distribution of internal pipe, $u = 2u_m\left(1 - \frac{r^2}{r_o^2}\right)$ and assuming that flow is fully-developed, where $\frac{\partial T}{\partial x} = \frac{\partial T_m}{\partial x} = constant$, then the energy balance gives,

$$\frac{1}{r}\frac{\partial}{\partial r}\left(r\frac{\partial T}{\partial r}\right) = \frac{2u_m}{\alpha}\left(1 - \frac{r^2}{r_o^2}\right)\frac{\partial T_m}{\partial x} + \overline{u'\frac{\partial T'}{\partial x}} - \Phi_{dissp} \tag{22}$$

It is important to mention that the considered turbulent flow is statistically steady or steady in the mean variables which velocity and temperature time fluctuations is not zero and also averaged. Integrate Eq. (22) twice with $T(r_0) = T_s$ and $T(0) = finite$, boundary conditions, the solution from energy equation is,

$$T(r) = T_s - \frac{2u_m r_0^2}{\alpha}\left(\frac{3}{16} + \frac{1}{16}\frac{r^4}{r_0^4} - \frac{1}{4}\frac{r^2}{r_0^2}\right)\frac{\partial T_m}{\partial x} + turbulence + dissipation \tag{23}$$

Note that this research does not provide the reader to the rigorous derivation of turbulent solution of convection problems since such solution do exist only for a few special cases [22]. However, the essential phenomenology can be illustrated by extending the results of laminar cases which will arrive at the similar result as in [23]. Thus, take average of Eq. (23) in $r$, yields,

$$T_m = T_s - \frac{11}{48}\frac{u_m r_0^2}{\alpha}\frac{\partial T_m}{\partial x} + turbulence + dissipation \tag{24}$$

or in another form,

$$T_m - T_s = -\frac{11}{48}\frac{q'' D}{\lambda} + turbulence + dissipation \tag{25}$$

$$T_m - T_s = -\frac{11}{48}\frac{U(T_m - T_s)D}{\lambda} + turbulence + dissipation \tag{26}$$

Overall heat transfer coefficient can be developed and rearranged into

$$\frac{\lambda L_f}{K_f} + \frac{\lambda}{h} = -\frac{11}{48}D + turbulence + dissipation \tag{27}$$

or

$$\frac{L_f}{K_f} = -\frac{11}{48}Nu + turbulence + dissipation - \frac{1}{h} \tag{28}$$

Remember that $R_f = \frac{L_f}{K_f A}$, then,

$$R_f = -\frac{11}{48A}Nu + turbulence + dissipation - \frac{1}{hA} \tag{29}$$

For any general empirical formula for turbulent flow, Nusselt Number can be replaced as

$$R_f = MRe^c Pr^d + turbulence + dissipation - \frac{1}{hA} \tag{30}$$

As it is discussed by Incropera *et al.,* and Churchill, the constant $M$ and turbulence term in Eq. (24)-(30) are depend on considered fluid properties and geometries that can be adjusted by experimental data. In this case, the time-averaged of fluctuations is also considered with the combination of mechanical dissipation. It is then affecting fouling chemical reaction or it is directly depended on Arrhenius reaction constant as parametrization of the last three terms which is expressed by,

$$R_f = (NRe^c Pr^d + B)f(t)e^{-\frac{E}{RT}} \tag{31}$$

where we take $M = Nf(t)e^{-\frac{E}{RT}}$ and $f(t)$ will be determined later. Thus, by relating Eq. (20) and (31), deposition and removal terms of fouling resistance is confirmed to follow sigmoid-typed functions.

### *2.3 The Proposed Model*

In this section, we start to combine phenomenological model of fouling and Sigmoidal-Boltzmann. Consider, the model proposed by Nasr-Givi, by taking addition information that removal also depends on Arrhenius reaction term, let $\gamma = \kappa e^{-\frac{E}{RT}}$, Eq. (7) can be expressed as

$$\frac{dR_f}{dt} = \left(nsRe^{\beta} - \kappa sRe^{0.4}\right)\frac{1}{s}f(t)e^{\left(-\frac{E}{RT}\right)} \tag{32}$$

while Sigmoidal-Boltzmann equation in differential form is shown as in the following (response variable or Y-variable set as $R_f$),

$$\frac{dR_f}{dt} = (A_2 - A_1)\frac{e^{\frac{(t-t_c)}{b_s}}}{b_s\left(e^{\frac{(t-t_c)}{b_s}} + 1\right)^2} \tag{33}$$

Relate Eq. (32) and (33), it can be confirmed that,

$$A_1 = \kappa s R e^{0.4} \tag{34}$$

$$A_2 = n s R e^{\beta} \tag{35}$$

$$b_s = s \tag{36}$$

In this case, the exponential term is expanded as $\left(e^{\frac{(t-t_c)}{b_s}} + 1\right)^2 = e^{2\frac{(t-t_c)}{b_s}} + 2e^{\frac{(t-t_c)}{b_s}} + 1$, which approximation $\left(e^{\frac{(t-t_c)}{b_s}} + 1\right)^2 = e^{2\frac{(t-t_c)}{b_s}}$ is taken by assuming that $e^{2\frac{(t-t_c)}{b_s}} \gg 2e^{\frac{(t-t_c)}{b_s}} + 1$. Thus, proceeding further as,

$$\frac{e^{\frac{(t-t_c)}{b_s}}}{e^{2\frac{(t-t_c)}{b_s}}} = f(t)e^{\left(-\frac{E}{RT}\right)} \tag{37}$$

and we arrive at the following expression,

$$t_c = \frac{sE}{RT} \text{ and } f(t) = e^t \tag{38}$$

It is shown that the initial and final parameters, $A_1$ and $A_2$, depend on Reynolds number which the difference is correlated to empirical fitting coefficients. Available data shows that the influence of shear stress which is represented as removal terms in Eq. (2) and (6) is little significant. This indicates that the influence of chemical reaction to both deposition and removal terms affect the initial and final parameters, and should be at the comparable values as $t \to \infty$. At the growing state, the fouling deposition is generally much greater than its removal. Take an example when deposition is dominant, the curve tends to be linear if $b_s$ is large. This will be resulted in a larger s value because deposition term is mainly driven by physical parameter including energy activation, film temperature and Reynolds number. The time characteristics $t_c$ depends on energy activation which has unique properties for each crude oil. Bulk temperature is taken into account to represent the fluid temperature for initial deposition. The parameter $b_s$ is thus can be interpreted as a time constant characteristic of Sigmoidal-Boltzmann curve which control the growing state as,

$$R_f = A_2 + \frac{A_1 - A_2}{1 + e^{\left(\frac{t-t_c}{b_s}\right)}} = \left(n s R e^{\beta}\right) + \frac{(\kappa s R e^{0.4}) - \left(n s R e^{\beta}\right)}{1 + e^{\left(\frac{t-\left(\frac{sE}{RT}\right)}{s}\right)}} \tag{39}$$

Therefore, the parameters of the sigmoid-typed fouling model are physically justified from the derivation of the governing equations. The main parameters such as Reynolds Number, fluid bulk temperature and the activation energy will be calculated based on specific crude oil used in the validation.

## 3. Results

The proposed model is validated by actual crude oil data of Petronas crude preheat train. The preheat train schematic is shown in Figure 2 below which there are eleven heat exchangers in the network. Three heat exchanger configurations set crude oil flow in shell side, and the remaining are configured in tube side.

Physical parameters ($Re$ and $T_f$) are obtained from averaging each operational condition. The activation energy used in this study is 18 kJ/mol based on calculation. Generally, the value of activation energy ranges from 20-55 kJ/mol. Complex factors due to physical process, chemical reaction, crude composition, and temperature affect the activation energy. The result is under common range because physical process factor is not separated from analysis. In other words, all processes are naturally involved. Figure 3 shows the energy calculation in crude oil study.

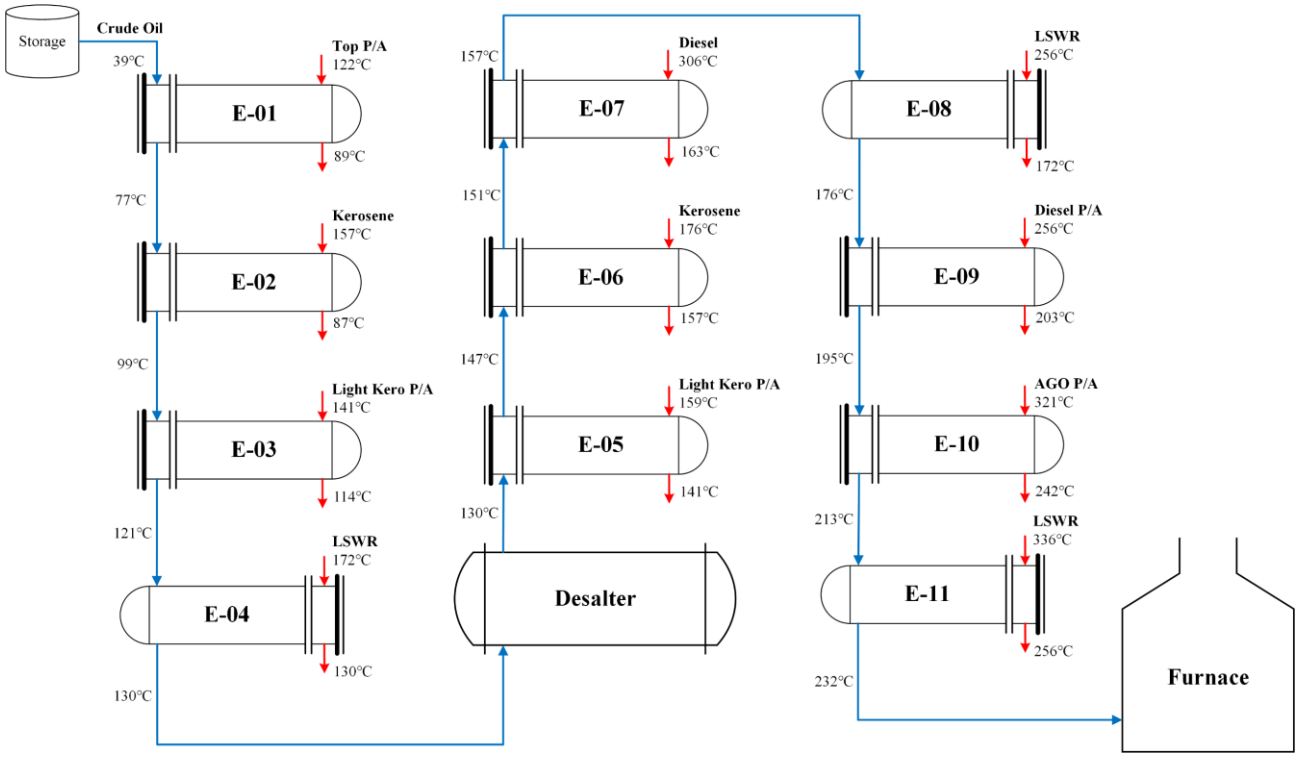


**Fig. 2.** Schematic diagram crude preheat train

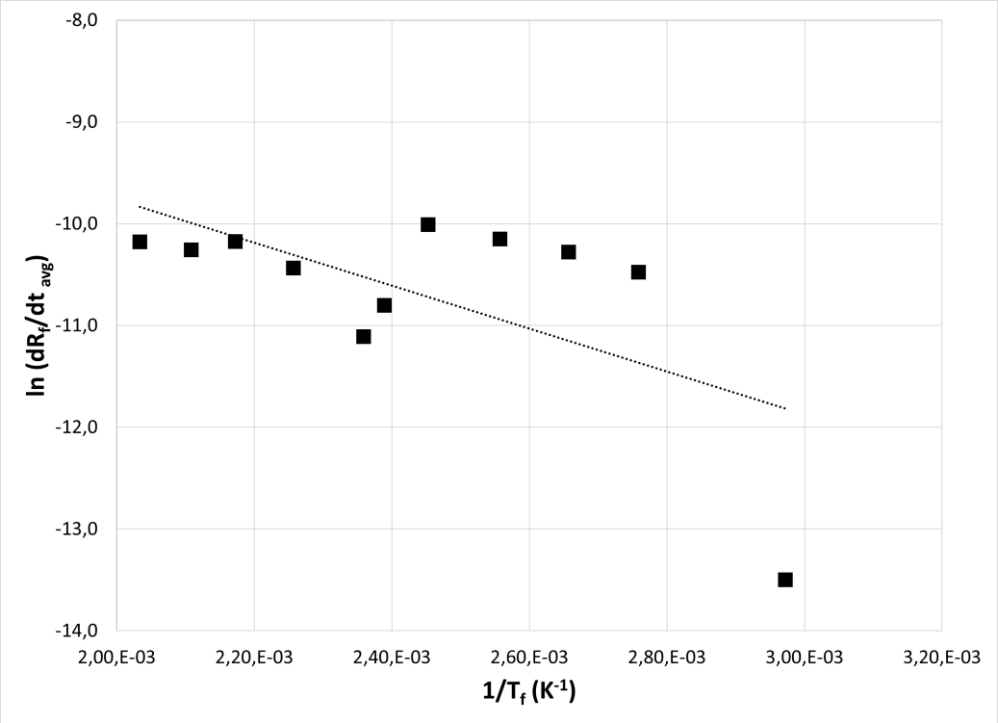


**Fig. 3.** Energy calculation in crude oil study

Note that film temperature in this study is approximated by average inlet-outlet crude temperature in each exchanger. Bulk temperature is calculated using the following formula [8],

$$T_b = \frac{1}{2}\left(T_{crude,in} + T_{crude,out}\right) \tag{40}$$

and wall temperature (used to calculate film temperature) can be approximated using [24],

$$T_w = T_b + \frac{q''}{h_{crude}} \tag{41}$$

Based on temperature profile data (Figure 4), this study shows that film temperature is near to bulk temperature with average increment about 3.8°C. It means that $q''/h_{crude}$ in wall temperature is not significant which $T_w \approx T_b$, such that $0.55(T_w - T_b)$ term in film temperature is neglected, resulted in $T_f$ equal to $T_b$.

After validating model with data by fitting, we classify each heat exchanger in three fouling resistance curves, i.e. exponential, sigmoidal, dan linear. There are four parameters of the proposed model (s, β, κ and n) (Table 1), each of which represents a Boltzmann Sigmoidal mathematical parameter associated with physical parameters, while the previous model has three parameters (n, β and γ). The constants s and β in all models have the same physical meaning, namely s is the deposition rate constant for the formation of fouling, while β is the Re power function for the deposition rate. Parameters κ and γ are removal rate constants which, the values are related to Arrhenius chemical reaction (besides Re) while in the previous model it only involved the Re factor (in the Nasr-Givi model) or shear stress (in the Polley model). The constant s is much larger than κ indicating the tendency of the fouling deposition process to dominate the removal process. A slight attenuation of deposition, thus causing a sigmoid or exponential curve, does not imply that

deposition is weaker than removal. However, the deposition was not strong enough to initiate a linear fouling trend in HE. In addition, the calculation results show that the value of κ is very small, so that in most cases the value is zero. This phenomenon can be interpreted that the removal process that occurs does not play a significant role in the process of developing fouling in HE as it is concluded in [18].

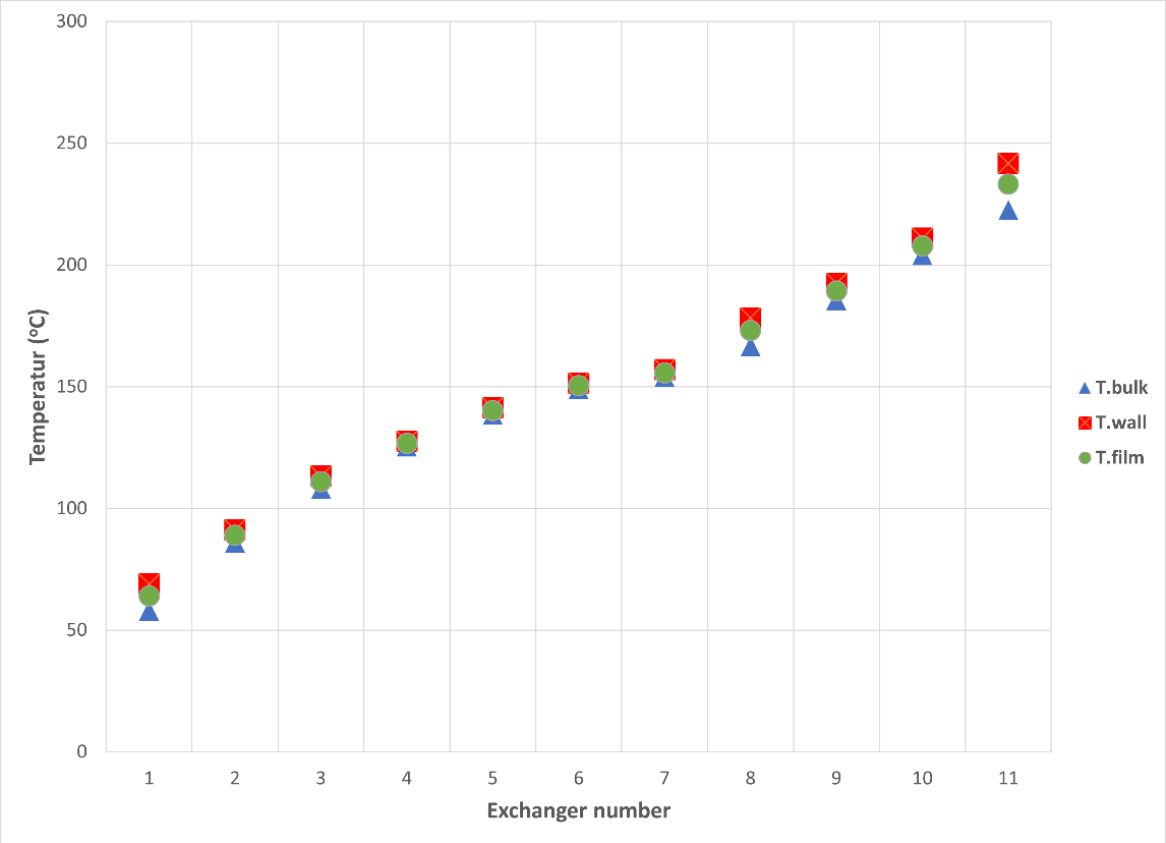


**Fig. 4.** Temperature profile

**Table 1**
Constant parameter of each heat exchanger

| No. | New Model Parameter | | | | Trend |
|---|---|---|---|---|---|
| | *1/s* | *β* | *κ* | n | |
| HE-01 | 3,29,E-03 | -0,63 | 6,27,E-10 | 0,14 | Exp |
| HE-02 | 3,77,E-02 | -0,48 | 0,00,E+00 | 0,07 | Exp |
| HE-03 | 4,70,E-02 | -0,46 | 1,60,E-06 | 0,11 | Sigm |
| HE-04 | 1,61,E-02 | -0,43 | 0,00,E+00 | 0,07 | Sigm |
| HE-05 | 1,97,E-02 | -0,44 | 0,00,E+00 | 0,11 | Sigm |
| HE-06 | 1,03,E-02 | -0,43 | 0,00,E+00 | 0,09 | Lin |
| HE-07 | 2,66,E-02 | -0,46 | 1,08,E-06 | 0,16 | Sigm |
| HE-08 | 2,66,E-02 | -0,44 | 0,00,E+00 | 0,24 | Sigm |
| HE-09 | 9,34,E-03 | -0,31 | 0,00,E+00 | 0,19 | Exp |
| HE-10 | 4,48,E-02 | -0,37 | 7,00,E-07 | 0,82 | Sigm |
| HE-11 | 2,89,E-02 | -0,39 | 0,00,E+00 | 0,22 | Sigm |

The other two parameters, namely β and n have different characteristics. The β value in all cases is negative and 0.44 in average, which has a correlation with the Re deposition rate. Higher Reynolds number implies decreasing fouling rate. While the value of n is related to the Arrhenius reaction of the deposition process which the dominating factor is T. Higher 1/T value, the smaller the n value.

However, the justification of the relationship between physical parameters and model parameters will be discussed further using the partial least squares (PLS) method.

Exponential HE fouling resistance curve are found in HE-01, HE-02, and HE-09. The exponential curve occurs because the fouling deposition process is stronger than the removal. In addition, the initiation phase occurs in a relatively short time (several days) so that in the initial phase of the HE operation it has entered the transport and deposition stages. Figure 5 shows the resistance curve exponential in HE-02.

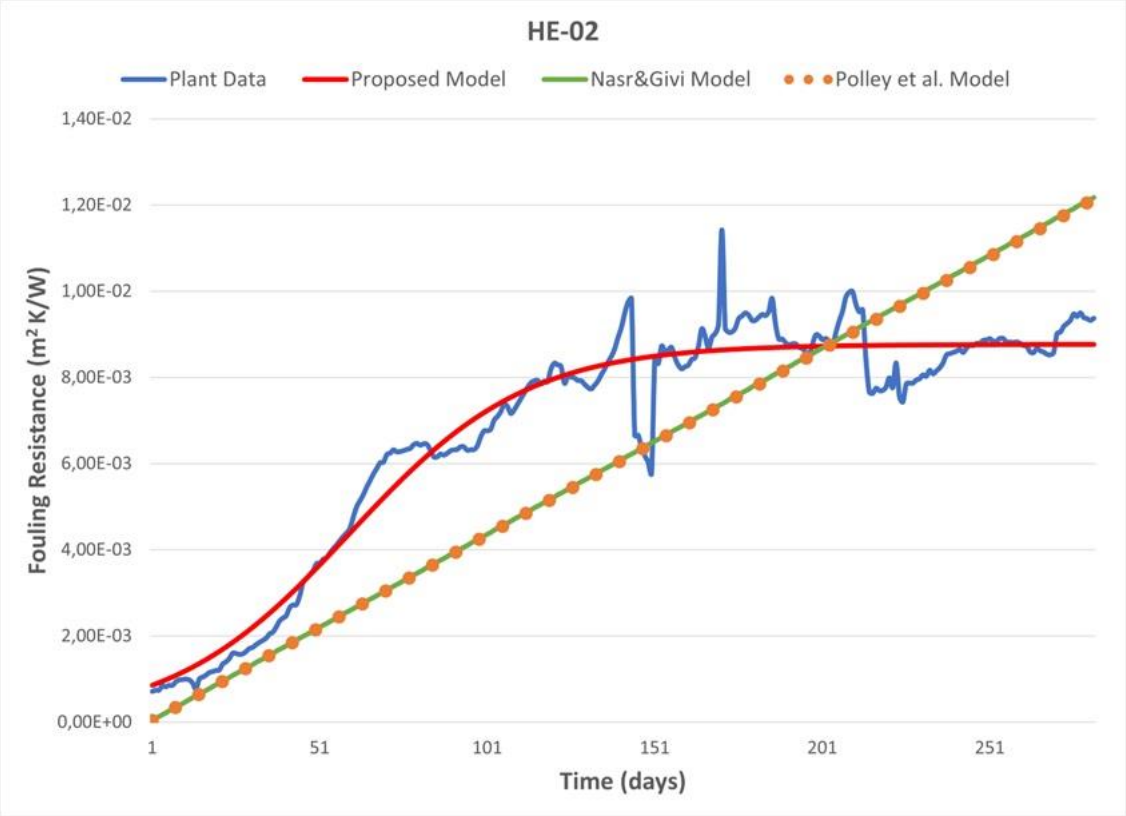


**Fig. 5.** Resistance curve exponential in HE-02

The character of the linear HE fouling resistance curve is found in HE-06 and HE-11. The linear trend is not purely linear like the previous models. It is categorized as linear because the slope of the curve around the midpoint of the sigmoid curve is quite large. The fouling characteristics of the two HEs explain the development process at the beginning of the operation period. Figure 6 shows the resistance curve linear in HE-06.

The sigmoidal HE fouling resistance curve characters are found in HE-03, HE-04, HE-05, HE-07, HE-08 and HE-10. Most of the fouling curve trends are sigmoidal, so it can be concluded naturally that fouling tends to be sigmoidal rather than linear (as claimed by previous models). The sigmoidal curve occurs with a similar explanation to the exponential, but the distinguishing characteristic is the longer initiation stage. Figure 7 shows the resistance curve sigmoidal in HE-08.

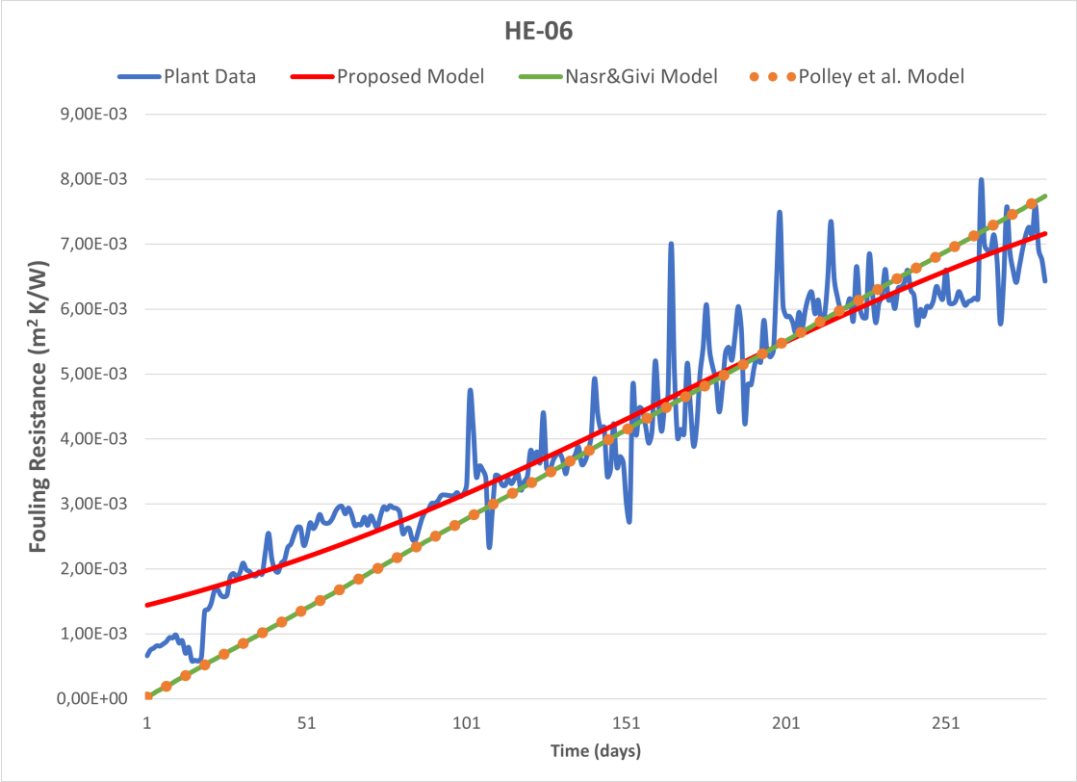


**Fig. 6.** Resistance curve linear in HE-06

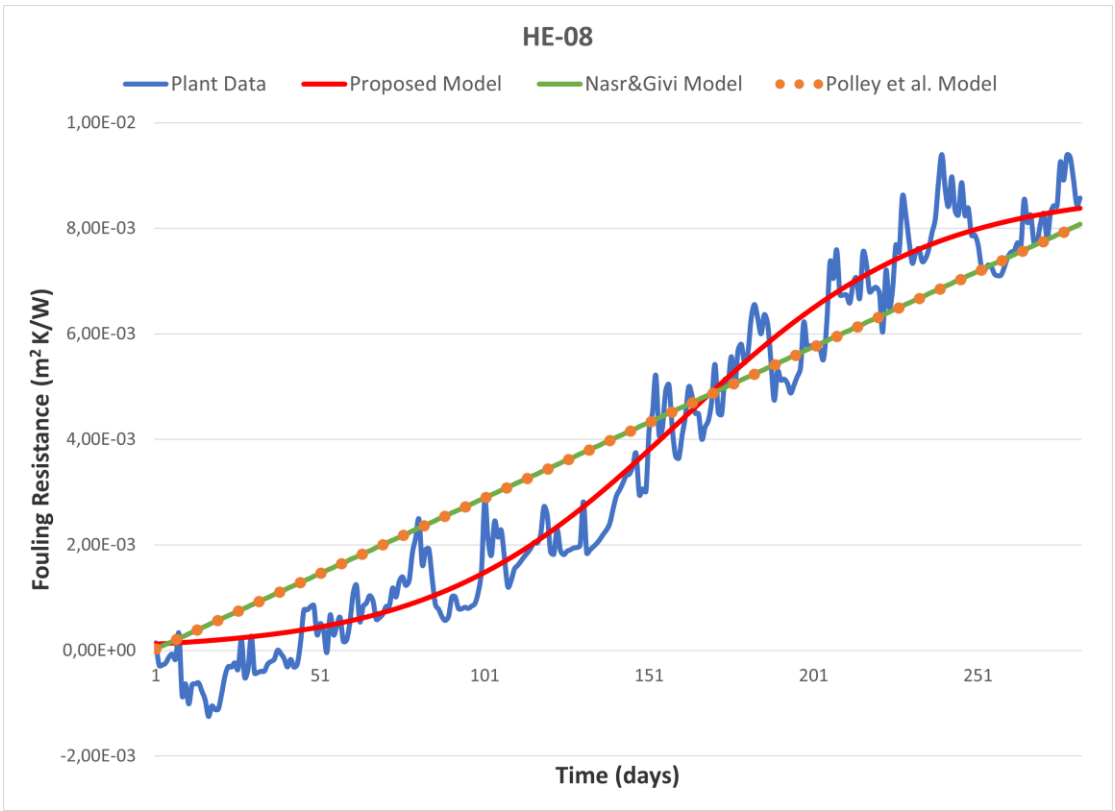


**Fig. 7.** Resistance curve sigmoidal in HE-08

Previous models only can predict linear curve tendency, but fails to represent sigmoidal and exponential. In overall, value $R^2$ shows better result in proposed model instead of previous model (Table 2). The proposed model is more flexible to capture non-linearity curve instead of previous models.

**Table 2**
Value of $R^2$ comparison Model

| | New Model | Previous Model |
|---|---|---|
| HE-01 | 76,42% | 67,14% |
| HE-02 | 94,99% | 46,19% |
| HE-03 | 87,02% | 27,70% |
| HE-04 | 94,15% | 82,85% |
| HE-05 | 96,16% | 93,56% |
| HE-06 | 92,79% | 84,76% |
| HE-07 | 88,16% | 7,55% |
| HE-08 | 96,25% | 87,88% |
| HE-09 | 98,44% | 97,60% |
| HE-10 | 96,67% | 73,58% |
| HE-11 | 86,84% | 86,26% |

Direct determination of each parameter dependencies and their influence on one another is difficult since some constants, such as s and κ have low sensitivity. Likewise, for example, the value of Re varies from one heat exchanger to another. In this case, the PLS statistical method is used to reveal the dependencies such that three principal components used in study to capture most of data variability (>0.8). It is calculated that the cumulative $R^2$ has reach a value of 0.835, while individual $R^2$ in each component is 0.232, 0.389, and 0.275 for first, second and third principal component, respectively. The result can be expressed in Figure 8 below, where fouling resistance as target variables, and the remains parameters is dependent variables. Comparing three of principal component needs to analyse graphical results in three plots, i.e. the first toward the second, the second toward the third, and the first toward the third. To simplify the analysis, we summarise into regression model which consist three principal component (one row represent one principal component), where *B* matrix is a weighting value of each variable.

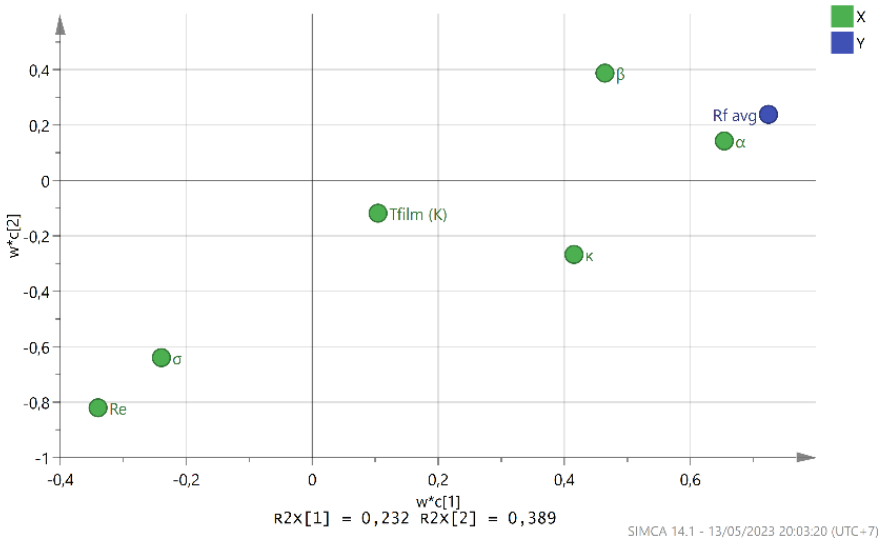


**Fig. 8.** Loading plot first principal component (X-axis) and the seconds principal component (Y-axis)

The results of the regression model formed from PLS can be written in mathematical form as follows,

$$\boldsymbol{Y} = \boldsymbol{Y_{const}} + \boldsymbol{XB} \tag{42}$$

where matrix $\boldsymbol{Y} = \begin{bmatrix} R_f[1] \\ R_f[2] \\ R_f[3] \end{bmatrix}$, $\boldsymbol{X} = [Re \quad T_f \quad \alpha \quad \beta \quad \kappa \quad \sigma]$,

$\boldsymbol{B} = \begin{bmatrix} -0{,}25 & -0{,}44 & -0{,}49 \\ 0{,}08 & 0{,}05 & 0{,}10 \\ 0{,}48 & 0{,}51 & 0{,}53 \\ 0{,}34 & 0{,}43 & 0{,}56 \\ 0{,}30 & 0{,}24 & 0{,}12 \\ -0{,}17 & -0{,}33 & -0{,}32 \end{bmatrix}$, and $\boldsymbol{Y_{const}} = \begin{bmatrix} 2{,}61 \\ 2{,}61 \\ 2{,}61 \end{bmatrix}$

and there are three regression outputs for each tested principal component. Parameters of $R_f$ and $s$ tend to always close each other (redundant) in all principal component scenarios. This means that $R_f$ highly depends on $s$ with positive correlation. This result consistent with the previous fitting result, where $s$ that represent deposition process is more dominant than removal. Another result regarding physical variables shows that $R_f$ also negatively correlated with Re. It means that higher Re value leads to lower $R_f$. Note that Re linearly depends on flowrate which, that higher flowrate causes reducing fouling resistance because removal process is slightly involved. Several variables, such as $n$ dan Re, have small correlation. The constants $\beta$ and $\kappa$ are weakly correlated though it must be positively correlated. It is similar to bulk temperature $T$ which has a weaker effect to fouling formation.

Ebert-Panchal model using laboratory and pilot data plant within film temperature range of 370-400℃ [25]. Polley *et al.,* and Nasr-Givi used the same refinery data, i.e. from Knudsen test, Exxon refinery data, Shell Wood River refinery data, and Shell Westhollow data [5,6]. These data recorded bulk temperatures of 223-371℃ and surface temperatures of 232-467℃. Farahbod-Karazhian also using Exxon refinery data in their model [10]. Shetty *et al.,* used their experimental rig data, capturing fouling in film temperature range about 177-263℃[8]. Deshannavar-Ramasamy used bulk temperature in range of 80-100℃ to study fouling characteristics [9]. The concern of previous works is using narrow range of temperature especially in high degree temperatures. It is not practical because the operational temperature starts from low (near ambient temperature) to high (before entering furnace), in the actual crude preheat train. It is supported by Petronas data which is ranging from 39 to 232℃.

## 4. Conclusions

The fouling formation is described by sigmoid-type function in this research. The model validity is compared to other models by fitting and adjusting its coefficients against the wide range data. It is found that the results are consistent with previous fitting, where $s$ that represent deposition process is much dominant than removal. Regarding to physical variables, it is shown that $R_f$ is negatively correlated with Re which means that the higher Re leads to lower $R_f$.

It is also concluded that using bulk temperature is simpler and more applicable compared to film temperature, because it needs measurement of wall temperature in the first place. On the other

hand, bulk temperature is widely known and easy to measure because has a direct relation with inlet-outlet crude temperature in each heat exchanger.

## Acknowledgement
This research was not funded by any grant.

## References
[1] Jradi, Rania, Christophe Marvillet, and Mohamed Razak Jeday. "Fouling in industrial heat exchangers: Formation, detection and mitigation." *Heat Transfer; Kazi, SN, Ed.; Open access peer-reviewed chapter* (2022). https://doi.org/10.5772/intechopen.102487

[2] Wu, Yan, Yufei Wang, Ruonan Liu, and Xiao Feng. "Applying plate heat exchangers in crude preheat train for fouling mitigation." *Chemical Engineering Research and Design* 165 (2021): 150-161. https://doi.org/10.1016/j.cherd.2020.10.023

[3] Ghorbani, Mahdi, and Reza Maddahian. "Investigation of asphaltene particles size and distribution on fouling rate in the crude oil preheat train." *Journal of Petroleum Science and Engineering* 196 (2021): 107665. https://doi.org/10.1016/j.petrol.2020.107665

[4] Awais, Muhammad, and Arafat A. Bhuiyan. "Recent advancements in impedance of fouling resistance and particulate depositions in heat exchangers." *International Journal of Heat and Mass Transfer* 141 (2019): 580-603. https://doi.org/10.1016/j.ijheatmasstransfer.2019.07.011

[5] Ebert, W., and C. B. Panchal. *Analysis of Exxon crude-oil-slip stream coking data*. No. ANL/ES/CP-92175; CONF-9506406-3. Argonne National Lab. (ANL), Argonne, IL (United States), 1995.

[6] Polley, Graham T., D. I. Wilson, B. L. Yeap, and S. J. Pugh. "Evaluation of laboratory crude oil threshold fouling data for application to refinery pre-heat trains." *Applied Thermal Engineering* 22, no. 7 (2002): 777-788. https://doi.org/10.1016/S1359-4311(02)00023-6

[7] Nasr, Mohammad Reza Jafari, and Mehdi Majidi Givi. "Modeling of crude oil fouling in preheat exchangers of refinery distillation units." *Applied thermal engineering* 26, no. 14-15 (2006): 1572-1577. https://doi.org/10.1016/j.applthermaleng.2005.12.001

[8] Shetty, Nitin, Umesh Basanagouda Deshannavar, Ramasamy Marappagounder, and Rajashekhar Pendyala. "Improved threshold fouling models for crude oils." *Energy* 111 (2016): 453-467. https://doi.org/10.1016/j.energy.2016.05.130

[9] Deshannavar, Umesh B., and Ramasamy Marappagounder. "Revisiting threshold fouling models for crude oil fouling." *Heat Transfer Engineering* 42, no. 17 (2021): 1489-1505. https://doi.org/10.1080/01457632.2020.1800276

[10] Farahbod, Farshad, and Neda Karazhian. "Presentation of Farahbod-Karazhian equation as an accurate mathematical model based on thermodynamics and fluid flow with the aim of predicting the deposition rate of oil heavy compounds in heat exchangers." *Energy Sources, Part A: Recovery, Utilization, and Environmental Effects* (2021): 1-12. https://doi.org/10.1080/15567036.2021.1955047

[11] Singh, Pragya, Srinivas Krishnaswamy, K. N. Ponnani, Ankur Verma, and Jaya Rawat. "Corrosion fouling during crude oil flow on a heated surface: Effects of temperature, shear and material of construction." *Heat and Mass Transfer* (2023): 1-16. https://doi.org/10.1007/s00231-023-03386-4

[12] Smith, Aaron D., and Emmanuel Hitimana. "Incorporation of fouling deposit measurements in crude oil fouling testing and data analysis." *Heat and Mass Transfer* (2023): 1-11. https://doi.org/10.1007/s00231-023-03388-2

[13] Rehman, Obaid ur, Marappa Gounder Ramasamy, Nor Erniza Mohammad Rozali, Shuhaimi Mahadzir, Ali Shaan Manzoor Ghumman, and Abdul Hannan Qureshi. "Modeling Strategies for Crude Oil-Induced Fouling in Heat Exchangers: A Review." *Processes* 11, no. 4 (2023): 1036. https://doi.org/10.3390/pr11041036

[14] Patil, Prafulla D., Mike Kozminski, John Peterson, and Sailesh Kumar. "Fouling diagnosis of pennsylvania grade crude blended with opportunity crude oils in a refinery crude unit's hot heat exchanger train." *Industrial & Engineering Chemistry Research* 58, no. 38 (2019): 17918-17927. https://doi.org/10.1021/acs.iecr.9b03921

[15] Ishiyama, E. M., S. J. Pugh, and D. I. Wilson. "Incorporating deposit ageing into visualisation of crude oil preheat train fouling." *Process Integration and Optimization for Sustainability* 4 (2020): 187-200. https://doi.org/10.1007/s41660-019-00104-8

[16] Biyanto, Totok R., M. Ramasamy, Azamuddin B. Jameran, and Henokh Y. Fibrianto. "Thermal and hydraulic impacts consideration in refinery crude preheat train cleaning scheduling using recent stochastic optimization methods." *Applied Thermal Engineering* 108 (2016): 1436-1450. https://doi.org/10.1016/j.applthermaleng.2016.05.068

[17] Saunders, E. A. D. "Heat Exchangers: Selection, Design and Construction, 1988." 528.
[18] Saleh, Zaid S., R. Sheikholeslami, and A. P. Watkinson. "Fouling characteristics of a light Australian crude oil." *Heat transfer engineering* 26, no. 1 (2005): 15-22. https://doi.org/10.1080/01457630590890049
[19] Berce, Jure, Matevž Zupančič, Matic Može, and Iztok Golobič. "A review of crystallization fouling in heat exchangers." *Processes* 9, no. 8 (2021): 1356. https://doi.org/10.3390/pr9081356
[20] Avanzini, Francesco, Gianmaria Falasco, and Massimiliano Esposito. "Thermodynamics of chemical waves." *The Journal of Chemical Physics* 151, no. 23 (2019). https://doi.org/10.1063/1.5126528
[21] Incropera, Frank P., David P. DeWitt, Theodore L. Bergman, and Adrienne S. Lavine. *Fundamentals of heat and mass transfer*. Vol. 6. New York: Wiley, 1996.
[22] Clark, Daniel, Richard DJG Ho, and Arjun Berera. "Effect of spatial dimension on a model of fluid turbulence." *Journal of Fluid Mechanics* 912 (2021): A40. https://doi.org/10.1017/jfm.2020.1173
[23] Churchill, Stuart W. "New simplified models and formulations for turbulent flow and convection." *AIChE journal* 43, no. 5 (1997): 1125-1140. https://doi.org/10.1002/aic.690430502
[24] Ahn, Taehwan, Jinhoon Kang, Jae Jun Jeong, and Byongjo Yun. "Measurement of local wall temperature and heat flux using the two-thermocouple method for a heat transfer tube." *Nuclear Engineering and Technology* 51, no. 7 (2019): 1853-1859. https://doi.org/10.1016/j.net.2019.05.007
[25] Panchal, C. B., W. C. Kuru, C. F. Liao, W. A. Ebert, and J. W. Palen. "Threshold conditions for crude oil fouling." *Understanding Heat Exchanger Fouling and its Mitigation* 273 (1999): 273-279.